STEWART, KIMBERLY D., M.S. Investigating the Role of Plasma Proteins in the Cellular Uptake of Metallic Nanoparticles. (2013)
Directed by Dr. Norman H.L. Chiu. 68 pp.

In recent years, applications of nanotechnology have increased at an unprecedented rate. Nanotechnology, which is the engineering of matter on an atomic and molecular scale, has proven beneficial in a number of scientific fields. In particular, nanotechnology has been credited with the use of nanoparticles for drug delivery and select nanomaterials have proven especially advantageous due to their highly variable functionalities and nontoxic nature [1].

Nanoparticles are characterized as being 1 to 100 nanometers in size, and are of great medical importance due to their unique characteristics. Each nanoparticle maintains a surface to mass ratio that is much larger than that of other particles. This allows compounds such as drugs, probes and proteins to bind to its surface. The nanoparticle is then able to carry the adsorbed substance throughout the body. Though it is certain that interaction occurs between nanoparticles and plasma proteins within the body, the extent to which they interact remains a matter of debate [2].

In this particular study the aim is to examine the role of plasma proteins in the cellular uptake of metallic nanoparticles. It is proposed that cellular uptake is predominantly driven by the presence of plasma protein; as such, increased uptake or adsorption is expected in the presence of a nanoparticle-plasma protein complex.

Examination of plasma proteins and their effects on the cellular uptake of nanoparticles will, in turn, advance the use and applications of nanomaterials.

INVESTIGATING THE ROLE OF PLASMA PROTEINS IN THE CELLULAR UPTAKE OF METALLIC NANOPARTICLES

by

Kimberly D. Stewart

A Thesis Submitted to
the Faculty of The Graduate School at
The University of North Carolina at Greensboro
in Partial Fulfillment
of the Requirements for the Degree
Master of Science

Greensboro
2013

Approved by

_____
Committee Chair

This degree and its inherent honor is owed to my closest friends and family—all of whom

have encouraged my persevering spirit

through their sincerest prayers, thoughts and deeds.

APPROVAL PAGE

This thesis written by Kimberly D. Stewart has been approved by the following committee of the Faculty of The Graduate School at The University of North Carolina at Greensboro.

Committee Chair _____
Dr. Norman H.L. Chiu

Committee Members _____
Dr. Gregory M. Raner

_____
Dr. Ethan W. Taylor

April 25, 2013
Date of Acceptance by Committee

April 25, 2013
Date of Final Oral Examination

ACKNOWLEDGEMENTS

I wish to acknowledge the faculty of Chemistry and Biochemistry—in particular, Dr. Norman Chiu who has served as my research mentor during the completion of both my second undergraduate and graduate degree(s) here at the university. I would also like to thank my thesis committee members, Dr. Raner and Dr. Taylor, both of whom extended intellectual guidance through their comments and suggestions.

Funding during my time here at the University of North Carolina at Greensboro was provided through the department, in the form of a graduate teaching assistantship, by way of the North Carolina Biotechnology Center and also through the National Science Foundation GK-12 Fellowship Program. I am incredibly thankful for each form of support and the academic development afforded through each experience.

Perhaps of most consequence is the support offered to me through the ever-encouraging persons I have the honor of calling friends and family. Through each trial and set-back these individuals have been unwavering in faith and have, time and again, prompted my persistence and believed in my success. I thank God for their presence throughout this intellectual journey.

TABLE OF CONTENTS

Page

LIST OF TABLES

Page

LIST OF FIGURES

Page

CHAPTER I

NANOTECHNOLOGY: BACKGROUND AND SIGNIFICANCE

The use of nanomaterials, including nanoparticles in medicine and industrial products, has exponentially increased over the past few years. According to the National Institute of Health, the global demand for nanomaterials and nano-enabled devices is expected to exceed $3.1 trillion by 2015. This branch of technology, which is confined to materials having nanoscale features, has peeked interests and investments in research and development (R&D) (Figure 1). In fact, nanotechnology—more so than any other technological field—has benefitted from substantial R&D investments, both public and through the private sector [3] (Figure 2) .

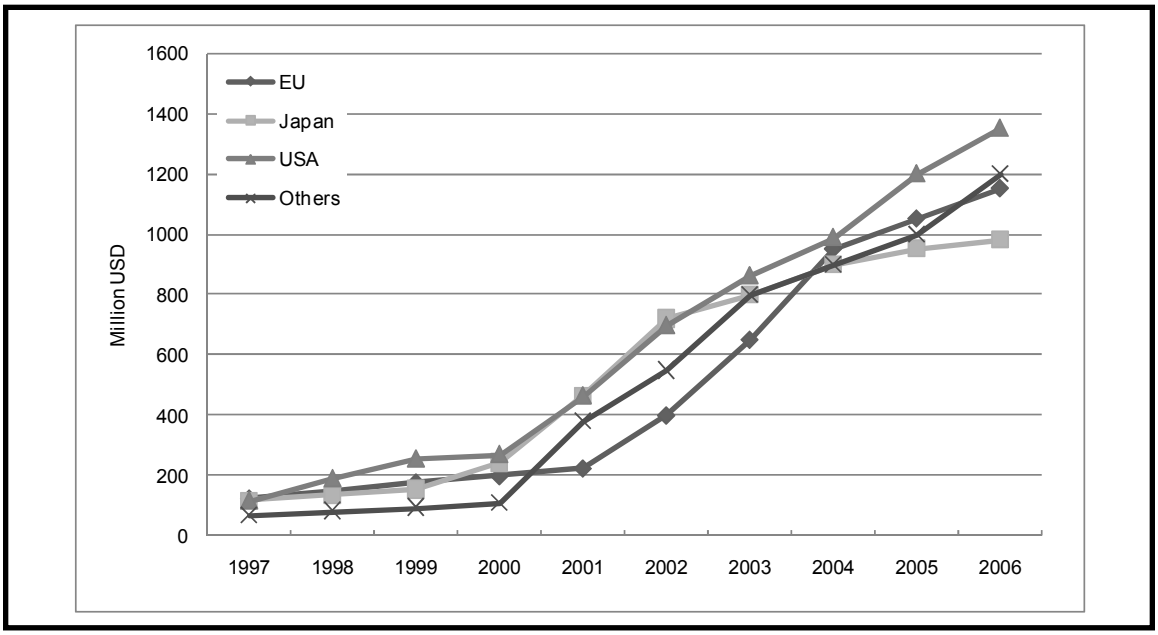

Figure 1. Public R&D Investments in Nanotechnology Globally [3]

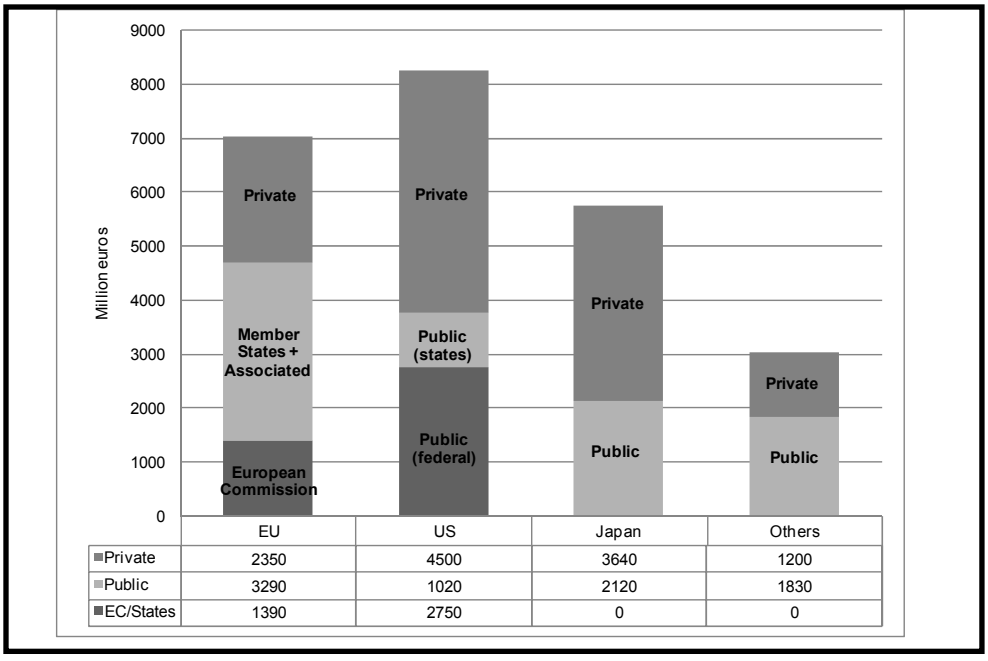

Figure 2. Structure of R&D Investments in the U.S., European Union (E.U.), and Japan by Institutional Sector, 2004-06 [4]

Investments in nanotechnology are further classified according to sub-area and patent data, the latter providing insight into the development and potential pathway of the field. The distribution of patents by field is outlined in Figure 3. Of the nanotechnological patents identified, the largest share is held by the nanomaterials sub-area—a division of particular interest in materials science.

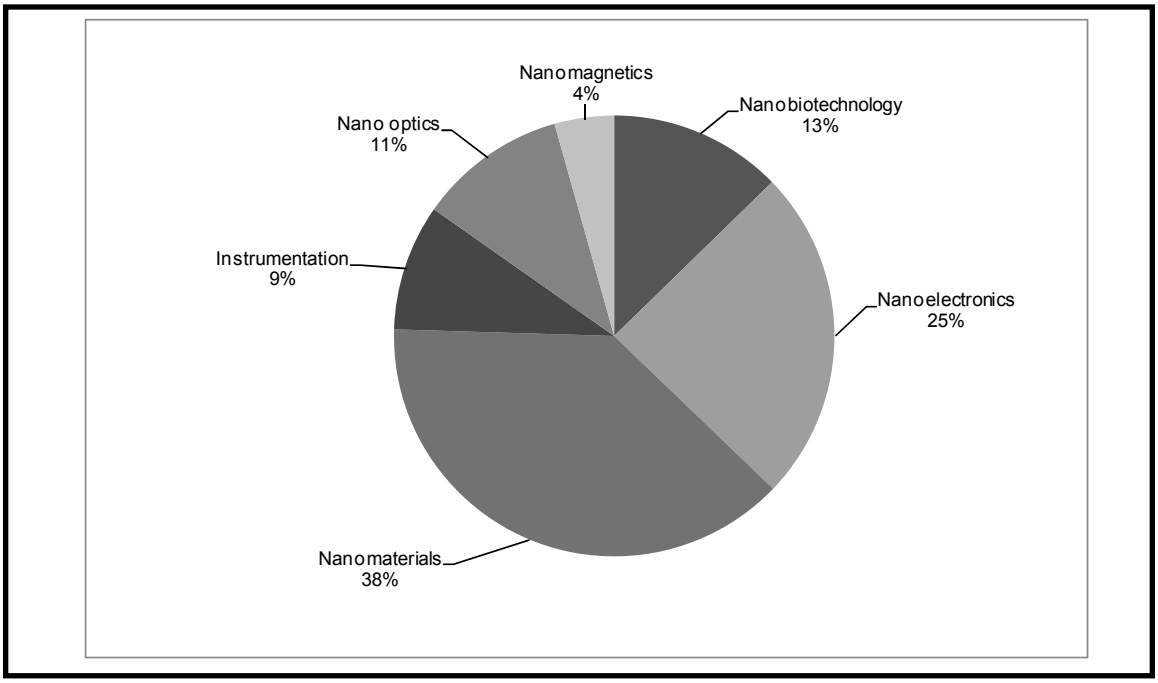

Figure 3. Share of Patents by Nanotechnology Sub-Areas [5]

CHAPTER II

NANOMATERIAL OF INTEREST: COLLOIDAL GOLD NANOPARTICLES

Gold nanoparticles (Au-NPs), which exist as a colloidal suspension, are nanometer-sized particles of gold. This nanomaterial has been used since 753 B.C.—initially for the purpose of glass staining [6]. It was not until the nineteenth century that colloidal gold was investigated for its scientific properties by Michael Faraday, at which time Au-NPs were discovered to have properties differing from bulk gold [7].

Further characterizing colloidal gold solutions, each was found to differ in hue according to the diameter of its suspended particles (Figure 4); solutions containing particles of 100 nm or less maintain an intense red color while those having diameters greater than 100 nm appear yellow. By taking advantage of variant nanoparticle sizes and their intrinsic interactions with light, each colloidal suspension can be tailored according to its optical properties and used in a number of applications. [8]

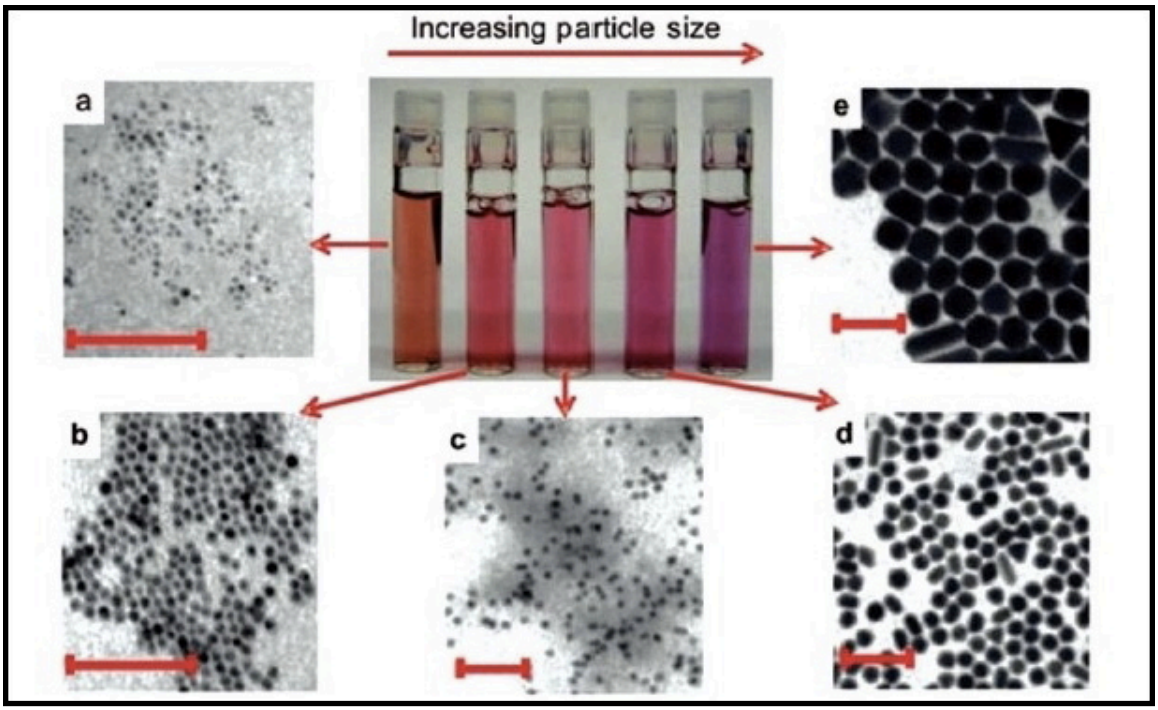

Figure 4. Aqueous Solutions of Gold Nanospheres as a Function of Increasing Dimensions [8]

Owing to their unique optical properties, Au-NPs maintain applicability in a number of disciplines including biological imaging, electronics and materials science. These optical properties can be tuned and used to treat and diagnose disease in either an indirect or direct manner. Furthermore, colloidal gold solutions can be tailored into various sizes, shapes and decorations, thereby affecting their functionality. This intrinsic characteristic has proven beneficial in biomedical applications, particularly targeted drug delivery systems (TDDS). [9]

Synthesis methods for Au-NPs were reported as early as 1951 by Dr. Turkevich who developed a 13 nm pivot synthesis, making way for current one-pot synthesis techniques. Facilitated one-pot synthesis procedures have led to the formation of nanoparticles ranging from 0.8 nm to 200 nm, the smallest of which have been shown to penetrate into cell nuclei and cross the blood brain barrier [9]. Ultra-fine nanoparticles have too been shown to bind various agents, probes and drugs, thereby serving as an effective delivery system for the treatment of cancerous cells and the like.

Colloidal Gold and Zeta Potential

Zeta potential (ζ) refers to the electrokinetic potential of a colloidal system and is quantified by the electric potential in the interfacial double layer of the colloid. A ζ-potential schematic for colloidal gold is shown in Figure 5.

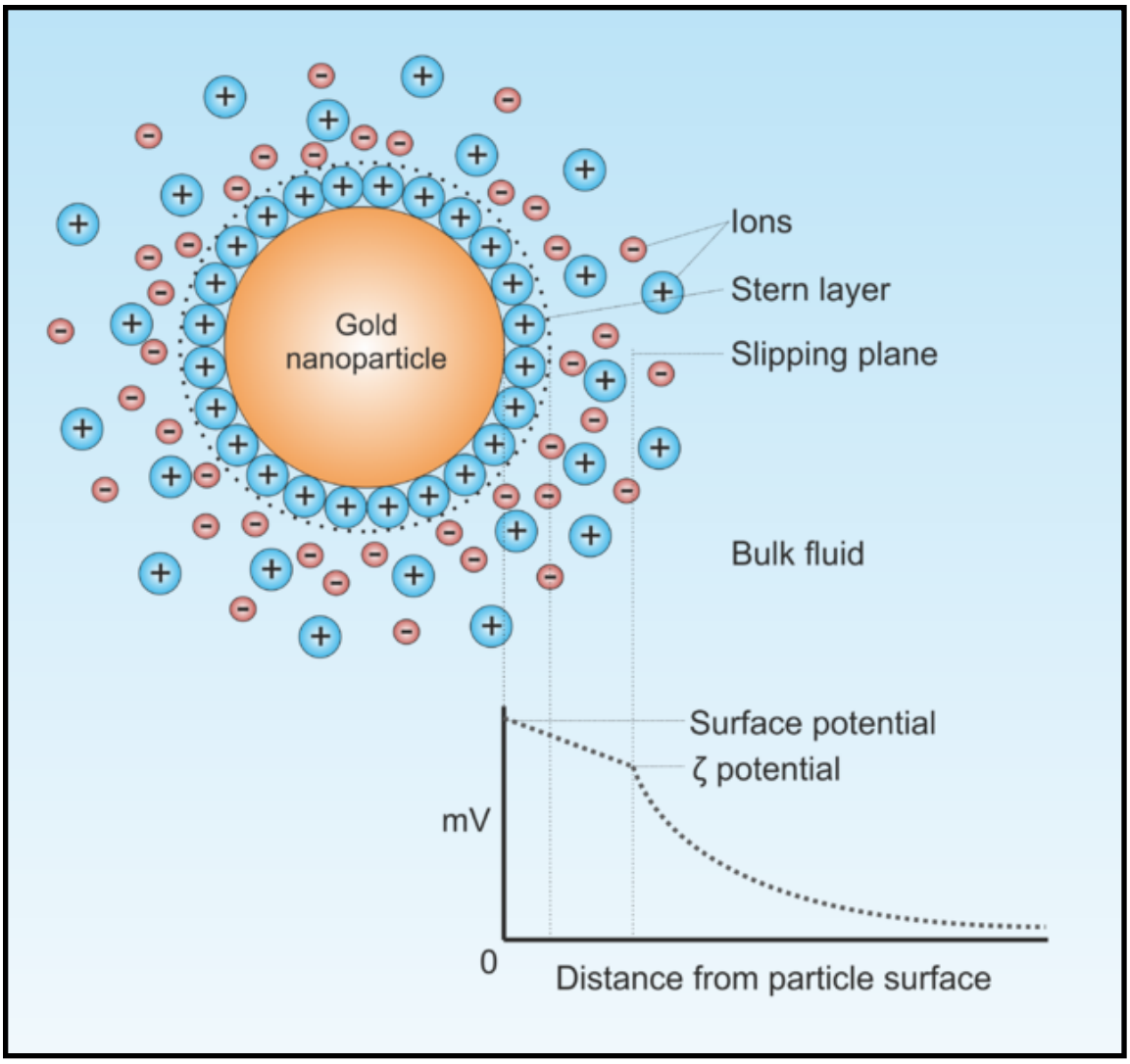

Figure 5. Zeta Potential Schematic of Colloidal Gold [10]

The double layer (DL) is comprised of two parallel layers of charge that surround the Au-NP. The first layer, or layer of charge that immediately surrounds the nanoparticle, is deemed the surface charge. It is made up of ions that are directly adsorbed onto the surface of the nanoparticle as a result of various chemical interactions.

The second layer maintains a detached attraction to the nanoparticle, as it is comprised of ions that are fluid, operating in accordance with electrical attraction and thermal motion. The ζ-potential is therein described by the electric potential in this interfacial double layer at the slipping plane versus a given point in the bulk fluid—the potential difference between the colloidal suspension of the Au-NP and the layer of fluid directly interacting with the particle defines the zeta potential.

Zeta potential values are used to classify the nature of colloidal suspensions, with a high ζ-potential—of magnitude 25 mV or more—indicative of stability and aggregative resistance (Figures 6 & 7).

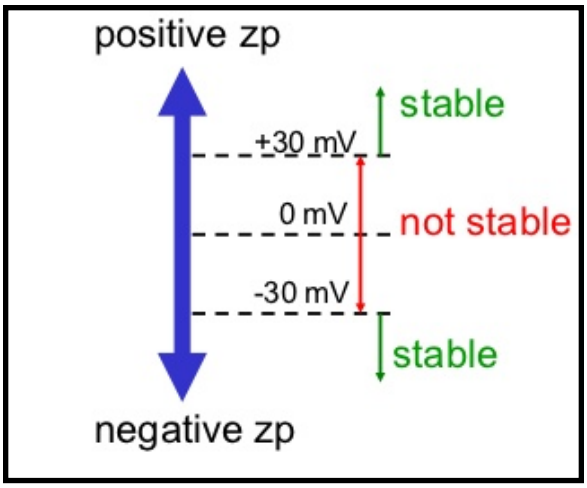

Figure 6. Zeta Potential and Stability [10]

Zeta potential [mV]	Stability behavior of the colloid
from 0 to ±5,	Rapid coagulation or flocculation
from ±10 to ±30	Incipient instability
from ±30 to ±40	Moderate stability
from ±40 to ±60	Good stability
more than ±61	Excellent stability

Figure 7. Zeta Potential and Stability [10]

Zeta potential reference measurements were performed by the National Institute of Standards and Technology (NIST) for 10 nm, 30 nm and 60 nm Au-NPs. Results indicate that 30 nm and 60 nm particles maintain ζ-potential values of -33 +/- 6.9 and -37.6 +/- 3.0, respectively [11]. Due to the intrinsically nanosized features of 10 nm Au-NPs, alongside their tendency to aggregate in solution, no ζ-potential value was definitively characterized.

Zeta potential, which is described according to the nature of a nanoparticle's surface charge and its surrounding solution, becomes increasingly complex to quantify in the presence of protein molecules. Protein molecule surface charges consist of unevenly distributed and complicated functions of amino acids and residues. Moreover, these charges are highly dependent upon the surrounding medium of the protein. In select modeling systems the interaction of proteins with charged surfaces has been shown to induce charge upon the protein molecule itself [2]. Adsorption studies of bovine serum albumin (BSA), a protein molecule of particular interest in this investigation, indicate changes in zeta potential—particularly at the protein's isoelectric point. Toward this end, interactions had by colloidal gold solutions and plasma proteins present an incredibly complex system as related to charge distribution.

CHAPTER III

PLASMA PROTEIN OF INTEREST: BOVINE SERUM ALBUMIN

Bovine Serum Albumin (BSA) is a large globular protein having a molecular weight of 66.5 kDa. It is regarded as a very functional protein, readily binding fatty acids and other lipids. This macromolecule is reported to partially unfold between 40 - 50 ˚C, thereby exposing its surface layer non-polar residues and enabling reversible protein-protein interactions [12]. BSA, one of the most widely used plasma proteins in research, is commonly added to solutions in order to stabilize enzymatic reactivity. Owing to its relatively neutral characteristics, BSA does not interfere with the enzyme of interest.

Albumin proteins are known to be amongst the smallest and most abundant plasma proteins within blood, indicative of the many metabolic compounds and therapeutic drugs for which they are responsible in transporting. These plasma proteins maintain a very high stability at select pH ranges (4-9) and below 60 ˚C. Furthermore, these proteins have demonstrated preferential uptake in tumor and inflamed tissue, biodegradability, low toxicity, immunogenicity and, with a half-life of 19 days, prove to effectively circulate within the blood [13]. Albumin proteins exhibit high binding capacities as a result of multiple drug binding sites and, as such, have been deemed an ideal drug carrier.

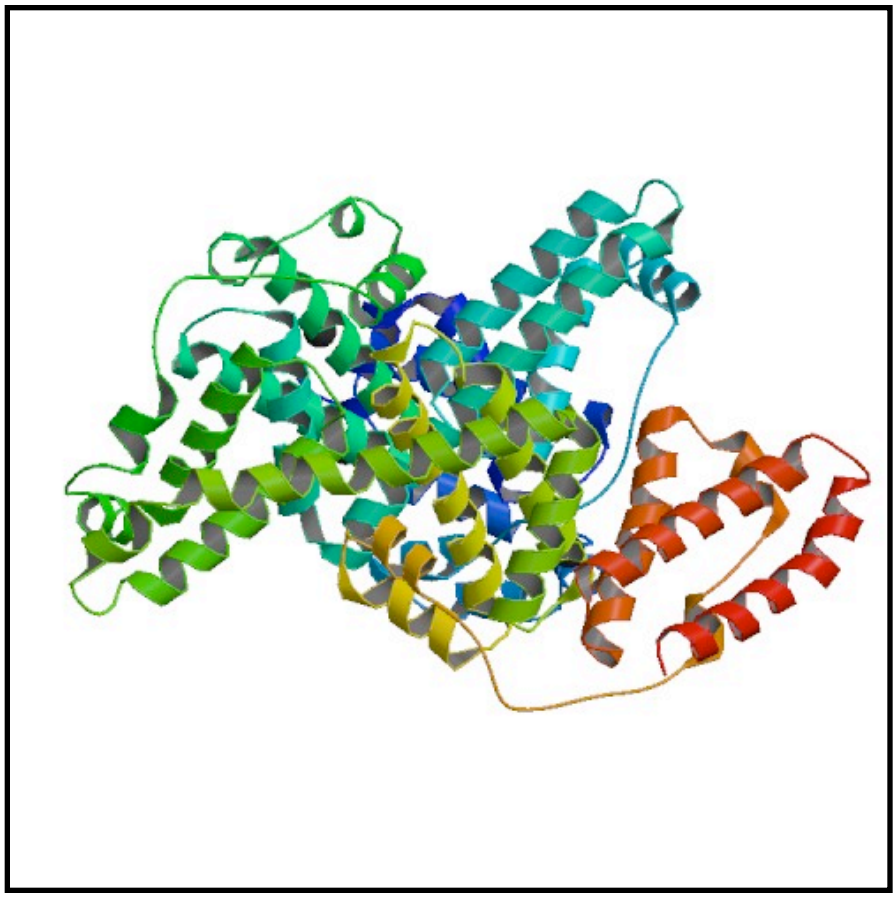

Figure 8. Bovine Serum Albumin, Crystal Structure [14]

Globular proteins, as is BSA (Figure 8), retain their structure in the presence of particles having increased surface curvature [2]. Surface curvature, which is an inherent property of nanosized particles, increases with decreasing particle size. A recent molecular interactions study of proteins and nanoparticles proposed information concerning the adsorption of BSA to Au-NPs. In this investigation BSA was adsorbed to the surface of hydrophilic Au-NPs, ranging 10 - 20 nm in diameter. In each case BSA was shown to retain its native-like structure. In alternate studies, however, the adsorption of biological molecules onto the surface of nano-structures yielded dissimilar results.

Under identical conditions and particle diameters, the secondary structure of proteins was disturbed, resulting in aggregation of the protein molecule. In turn, the nano-bio interface is regarded as an elaborate arrangement and heavily investigated in terms of its molecular dynamics.

CHAPTER IV

THE NANOPARTICLE-PROTEIN INTERFACE

Nanoparticle-protein conjugates (Figure 9) maintain applicability in sensing, self-assembly and imaging techniques. Their usefulness in these types of applications, however, is dependent upon the site-specific adhesion of protein to the nanoparticle of interest. Binding should occur in a way so as not to interfere with the structure nor function of the protein. This is difficult to achieve. Both nanoparticles and proteins are incredibly complex chemical systems and interact by way of numerous non-covalent interactions. As a result, the nanoparticle-protein interface is not well understood and is a major barrier in terms of biological applications. [15]

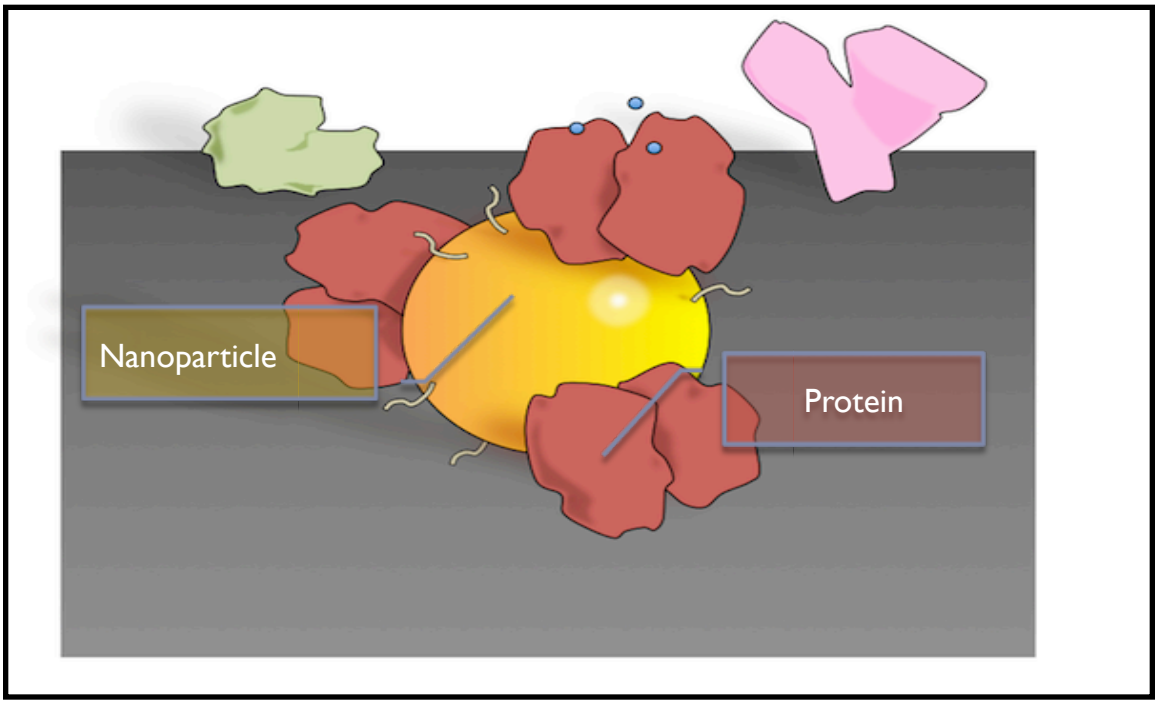

Figure 9. Nanoparticle-Protein Interface [15]

The Nanoparticle-Protein Corona Theory

While the nature of the nanoparticle-protein interface is yet to be fully understood, it is increasingly accepted that the surface of nanoparticles—in biological environments—is modified by the adsorption of biomolecules, namely proteins and lipids [16]. This biomolecular interface is characterized as either a hard or soft protein corona (Figure 10), each category indicative of nanoparticle-protein adhesion rates. The lifetime of the hard protein corona is believed to be for many hours and stable enough to govern the biological identity of the nanoparticle to which it is adsorbed.

In a typical biological environment, there are a number of biomolecules competing for adsorption to a limited nanoparticle surface. Thus, the nanoparticle-protein corona is dependent upon the ratio of available nanoparticle surface area to surrounding proteins [16]. In biological solutions the most abundant protein is immediately bound to the nanoparticle and later ejected from the corona to be replaced by proteins having a higher affinity for the nanoparticle. The identity of the corona is, in turn, dictated by protein-binding affinities and the intrinsic properties of the associated nanoparticle.

A study of the corona within varied biological environments points toward an evolution of the nanoparticle-protein corona (Figure 10) and its adaptive nature. The long-lived or "hard" corona is shown to re-equilibrate as the nanoparticle moves from one biological fluid to another. Within the second biological solution, the protein corona maintains a fingerprint of its history—though some proteins, having been initially adsorbed to the nanoparticle, are replaced by those in the new biological fluid a number of proteins in the original corona remain. [17]

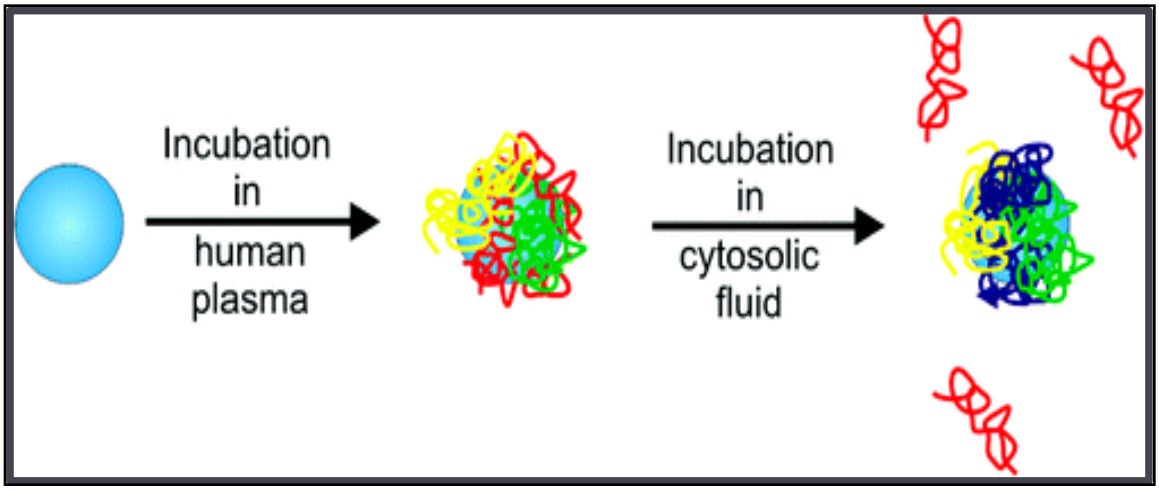

Figure 10. Evolution of the Nanoparticle-Protein Corona [17]

Although a direct comparison cannot be drawn in terms of the cellular uptake pathway, the nanoparticle-protein corona theory has major implications: 1) in a given biological solution nanoparticle-protein complexes form in a transient yet specific manner and 2) the nanoparticle-protein corona, if sufficiently long-lived, comes to dictate the biological fate of nanoparticles.

CHAPTER V

NANOPARTICLES AND CELLULAR UPTAKE

As nanoparticle applications continue to increase, as does the potential for incidental exposure and deliberate contact through targeted delivery systems and products [18]. Even with expanding interest in the field, the potential effects of nanoparticles on cellular systems and their resultant toxicity remains under investigated. Effects of nanoparticle exposure are dependent upon a number of quantifiable parameters—including cell type, nanoparticle dosage, composition, size, shape and surface chemistry—yet minimal studies have been performed that mathematically model or directly investigate the cellular uptake of nanoparticles. Though considerable work has been done in the quantitative analysis of cellular uptake and nanoparticles, elucidation of a pathway remains incomplete.

As such, no definitive models have been presented but rather a number of potential entry mechanisms (Figure 12). These include: 1) endocytosis, 2) diffusion and 3) channel, all of which are thought to occur by way of a nanoparticle-lipid bilayer interface (Figure 11).

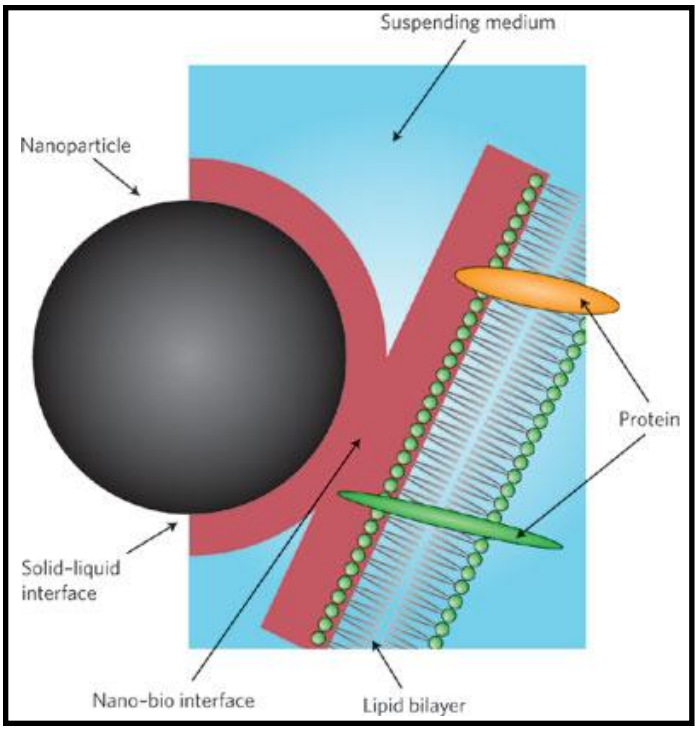

Figure 11. Nanoparticle and Lipid Bilayer Interface [19]

Potential Cellular Uptake Mechanisms

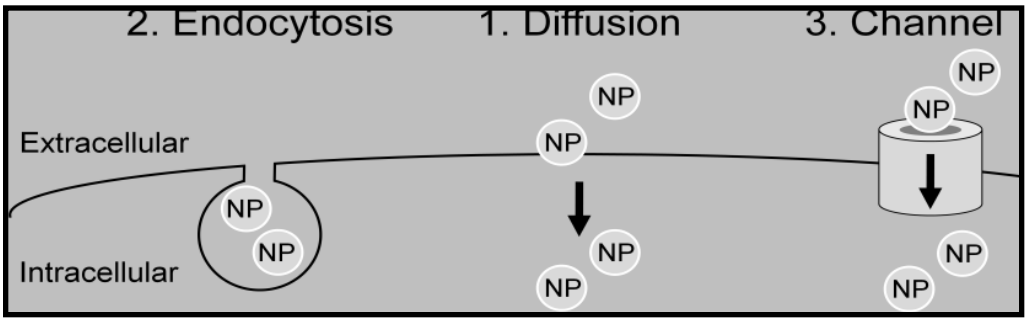

Figure 12. Potential Mechanisms of Nanoparticle Cellular Uptake [18]

1) Diffusion

The direct diffusion of nanoparticles across the cellular membrane is thought to occur in select pathways. This penetration of the lipid bilayer is, however, dependent upon a number of variables with regard to the nanoparticle of interest. The size, charge, hydrophobicity, composition and shape of a nanoparticle are believed to dictate the mechanism of uptake and, furthermore, depends upon the medium involved. The nanoparticle surface, solid-liquid interface and nano-bio interface (each of which is shown in Figure 11) characterize the biological environment and resulting behaviors. [18]

2) Endocytosis

Endocytosis refers to the engulfment of a particle within the lipid bilayer. This process is most often used to ingest very large or polar molecules that do not readily travel through hydrophobic medium or the cell membrane. Data suggests that the endocytosis pathway varies according to nanoparticle size and other such physical parameters. [19]

3) Channel

Though a number of ion channels and transporter proteins are contained within the plasma protein, they maintain a high level of selectivity and incredibly small pore sizes. In theory, these channels assist in the translocation of substances into and out of the cell. Each pore is aqueous and facilitates the rapid movement of molecules across the

cellular membrane. As is the case, only nanoparticles having extremely small or negligible diameters are thought to proceed by way of ion channels. [22]

CHAPTER VI

HYPOTHESIS AND SPECIFIC AIM

We propose that the cellular uptake of nanoparticles is, in some way, mediated by the presence of plasma protein. As such, our aim is to examine differences in cellular uptake between bare Au-NPs and plasma protein coated Au-NPs. In this study 10 nm Au-NPs will be used to form nanoparticle-plasma protein complexes with the commercially available bovine serum albumin protein (BSA). A representative schematic of our proposed investigation is pictured in Figure 13.

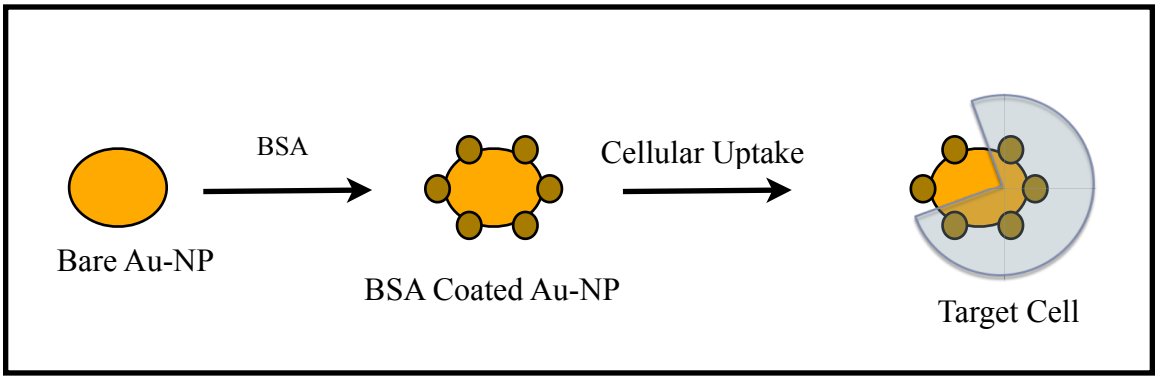

Figure 13. Examination of Protein-Coated Au-NP Cellular Uptake

It should be noted that, to date, there is no standard method with which to follow the cellular uptake of nanoparticles. As such, this study does not propose to lend

information pertaining to the *mechanism* of nanoparticle cellular entry but rather the *role* of plasma protein in the cellular uptake of Au-NPs.

Experimental Outline

Investigation of Au-NP cellular uptake will proceed in three stages:

1) Host Cell Formation and Lysis

2) Nanoparticle-Protein Complexation

3) Examination of Cellular Uptake

CHAPTER VII

HOST CELL FORMATION AND LYSIS

Objective - Host Cell Formation

For the purposes of this study, the Cytochrome P450 BMH-F87G: W96H cell line was acquired to use as a host for Au-NP delivery. This cell line contains a double-mutated plasmid obtained by way of a single mutation of the Trp96 codon on a previously mutated F87G plasmid that screened positive for the mutation [23]. The cell line is further characterized as a gram-negative *Escherichia coli* bacterial strain. It should be noted that bacterial versus mammalian cells were used in this study; bacterial cell lines are known to have less complex systems and greater reproducibility *In vitro*.

Experimental- Host Cell Formation

Growing nutrient used for the bacterial cell line was prepared by dissolving 47.6 g of Terrific Broth Medium (TBM), available from Sigma Aldrich, in 1 L of NANOpure water. The solution was then autoclaved in a Primus® system at 250 ˚F for a 16 minute sterilization time and then cooled to room temperature. An aliquot of the broth was treated with ampicillin (1 mg/ mL) to prevent cell culture contamination. Bacteria from the F87G cell line was added to the TBM aliquot at a dilution of 1.75 mL / 35 mL TBM.

Cells were incubated in a rotary shaker at 37˚C / 90 rpm and harvested at an optical density (OD) of 0.2 - 0.3, as measured by the Cary UV-Vis Spectrophotometer.

Experimental Results- Host Cell Formation

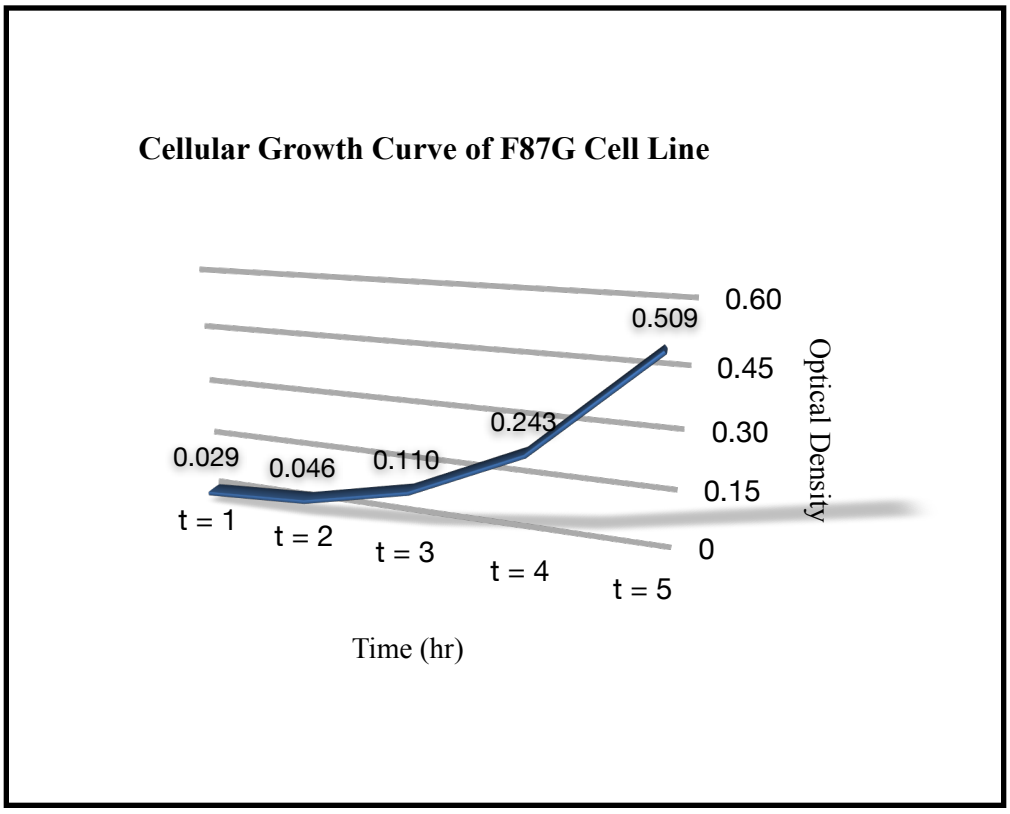

Figure 14. Cellular Growth of F87G Cells as a Function of Time

Objective - Lysis

In order to quantify the cellular uptake of Au-NP content, lysing procedures for the F87G cell line were examined. Noting the sensitivity of select nanoparticles, a non-chemical disruption technique was first explored, followed by a chemical digestion

approach. It should be noted that the Au-NPs used in this study were not compromised by chemical disruption methods.

Through both the chemical (nitric acid digestion) and non-chemical (sonication) lysing techniques employed, the aim was to disrupt the cells and to recover a maximal amount of cellular content. The lysate from each cellular sample would then be used to quantify the amount of Au-NPs ingested by F87G cells.

Results from the non-chemical digestion method are displayed in Figures 15 & 16 and discussed in detail in Chapter XI.

Experimental - Lysis

Three milliliters of cellular content were transferred to a 10 mL centrifuge tube and inserted into the Ultrasonic 3000 Homogenizer instrument. Instrument settings were varied according to pulsing speed, intensity and time (pulsing time did not exceed 5 min. in order to preserve cellular integrity). In order to determine cellular disruption percentage values, an initial OD measurement was recorded prior to sonication and a second OD value recorded following cellular disruption.

Experimental Results- Lysis

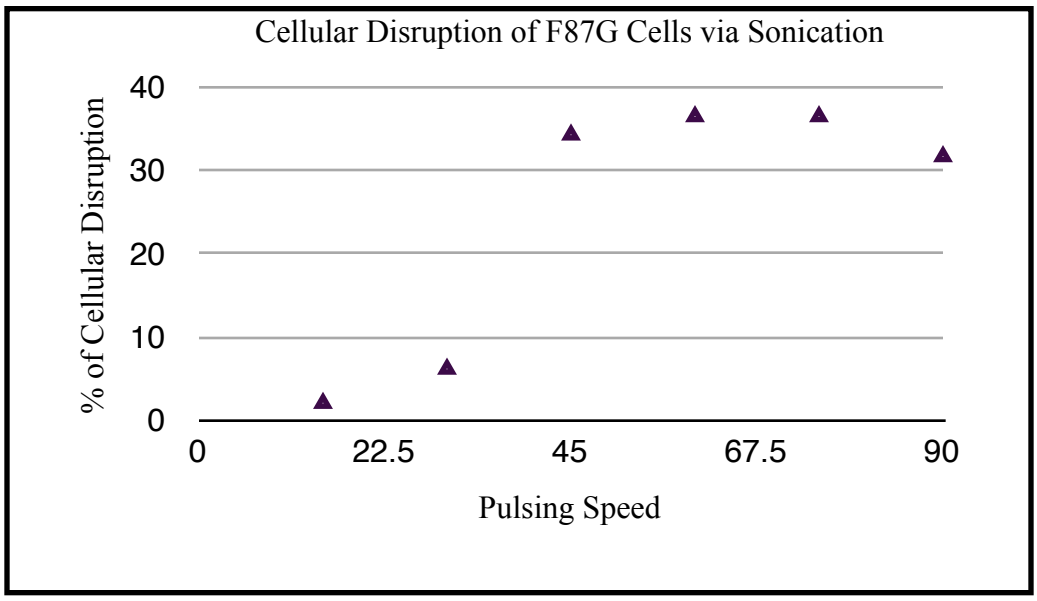

Figure 15. Percent of Cellular Disruption as a Function of Pulsing Speed

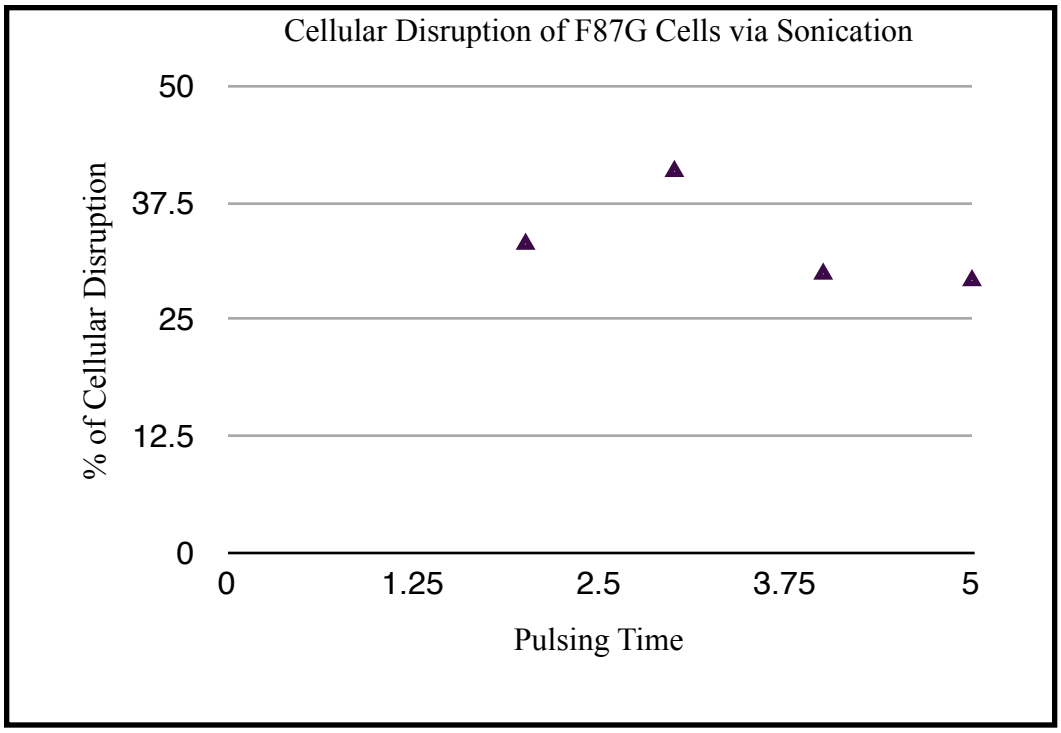

Figure 16. Percent of Cellular Disruption as a Function of Pulsing Time

CHAPTER VIII

NANOPARTICLE-PROTEIN COMPLEXATION

Summary of Results

According to work performed by researchers Lynch and Dawson, nanoparticles and proteins—when introduced into a biological environment—form a nanoparticle-protein complex [16]. As such, the complexation of Au-NP and protein was not further investigated in this study.

For the purposes of quantifying nanoparticle and protein complexation as related to experimental parameters, Au-NP and BSA were combined in solution. Following attempts to quantify the presence of Au-NP within the complex, our method of instrumentation (UV-Vis Spectrometry) proved inefficient—this technique was not sensitive enough to account for the intrinsic concentration of Au-NP being used. In turn, this portion of the study led to the examination of alternate methodology, at which time the Au-NP content within nanoparticle-protein complexes was indirectly quantified by way of cellular uptake studies.

CHAPTER IX

GRAPHITE FURNACE ATOMIC ABSORPTION SPECTROMETRY

Owing to the noted lack of sensitivity within UV-Vis Spectrometry techniques, alternate instrumentation was examined for its viability in measuring the presence of Au-NP content within cells. Considered methodologies included: 1) immunoassays, which posed an extensive effort in the location of appropriate antigen and antibody combinations, 2) mass spectrometry, also proving lengthy in regard to training and acquiring technical skill and 3) zeta potential, known for the characterization of colloidal solutions yet not an available departmental resource. The use of graphite furnace atomic absorption spectrometry (GFAAS), though not a standard way to measure the cellular uptake of colloidal gold, proved to be the most direct and readily available technique.

Background and Advantages

GFAAS is a form of spectrometry that utilizes a graphite-coated furnace to atomize sample contents. Atoms within the sample absorb light at wavelengths characteristic to the element of interest and, using this information, the concentration of analyte can be determined. These concentration measurements are determined by way of an internal calibration curve, as generated by the instrument prior to sampling.

The GFAAS technique is inherently more sensitive than that of UV-Vis Spectrometry, has greater detection limits, low spectral interference and requires a reduced quantity of sample.

Instrumentation

The GFAAS system used within this study was composed of the following basic features 1) an optimized Au lamp, which served as the source of light, 2) a graphite tube / atomization chamber wherein the sample is vaporized 3) a monochromator which selects for characteristic wavelengths of elemental Au, 4) a photo-multiplying detector and 5) a computing processor.

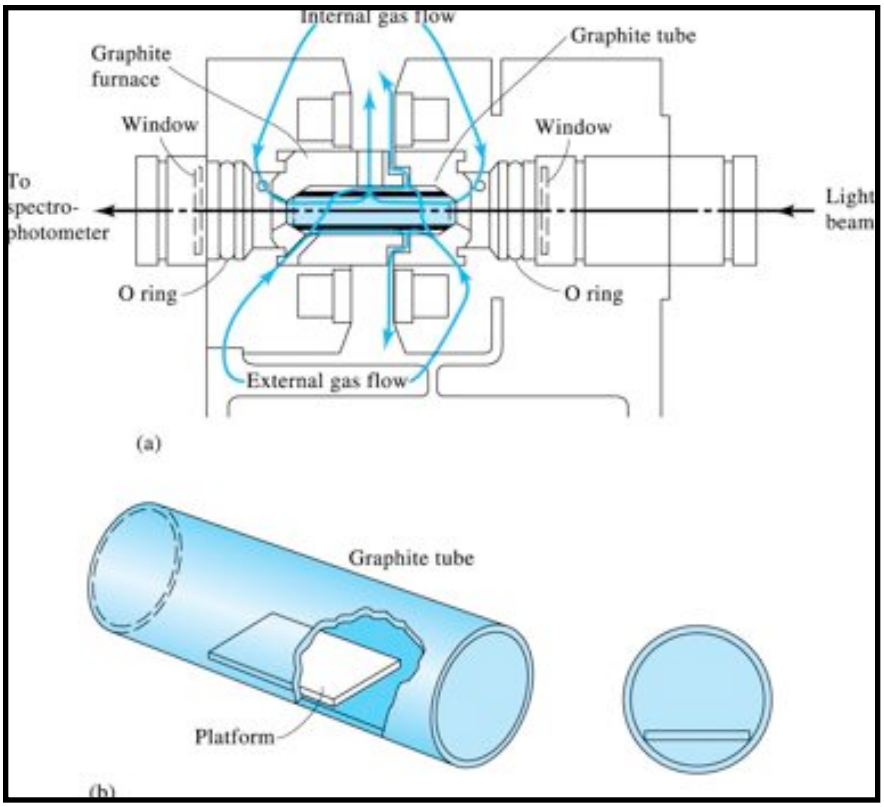

Figure 17. Graphite Furnace Atomic Absorption Spectrometer Schematic [24]

In order to achieve vaporization of the analyte, the GFAAS system operates according to a temperature programming system which gradually increases the furnace temperature with time. Figure 18 diagrams the temperature programming of the SpectrAA 220 FS GFAAS system used within this study and optimized for the analysis of Au-NP cellular uptake.

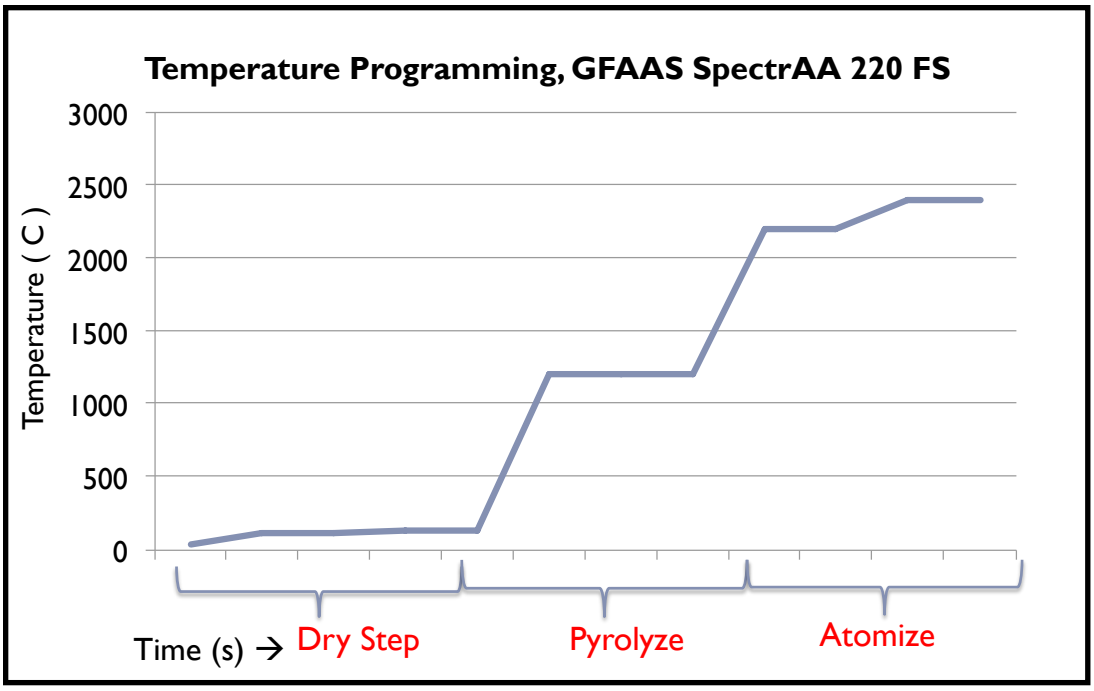

Figure 18. Temperature Programming of GFAAS SpectrAA 220 FS Instrument

CHAPTER X

EXAMINATION OF CELLULAR UPTAKE

Phase I - 50 nm Au-NP Studies

Objective

In this phase of cellular uptake examination, we aimed to differentiate cellular uptake from the centrifugal sedimentation of Au-NPs in solution. In doing so, we utilized our working knowledge of F87G cell centrifugation patterns. In prior studies, cellular content was shown to be sufficiently collected at 6000 rpm / 10 min. / 4 ˚C. In order to eliminate the possibility of Au-NPs being gravitationally depressed in solution versus ingested by cells, we sought to determine a centrifugation speed wherein Au-NPs remained suspended in solution while F87G cells were maximally collected.

Experimental

A 50 nm colloidal gold solution was obtained from nanopartz.com. It should be noted that 50 nm Au-NPs were first used for experimentation in order to develop a working knowledge of variant nanoparticle sizes in solution. Performing initial studies with a median-sized nanoparticle allowed for facilitated adjustment within the 1 - 100 nm particle range.

Four milliliters of 1X Phosphate Buffer Saline (PBS) were transferred to a 15 mL centrifuge tube and combined with 0.2 mL of 50 nm Au-NPs. This solution was gently inverted. The optical density of the solution was measured by way of UV-Vis Spectrometry at 530 nm. Solution contents were then centrifuged at conditions optimized for the collection of F87G cells. The optical density of the supernatant was remeasured following centrifugation in order to detect for Au-NPs remaining in solution.

Owing to the inherent lack of sensitivity yielded by UV-Vis Spectrometry measurements, these results were validated by way GFAAS. Again using 50 nm Au-NPs, 0.2 mL of colloidal gold solution was combined with 4.0 mL of PBS. Two 50 uL aliquots of the aforementioned solution were removed and digested overnight in 69% TraceSELECT HNO_3—a chemical digestion technique for Au-NPs validated in literature. Aliquot 1 was centrifuged at conditions optimized for the collection of F87G cells and Aliquot 2 was not centrifuged. GFAAS measurements were performed in order to detect for Au-NPs remaining in solution.

Experimental Results

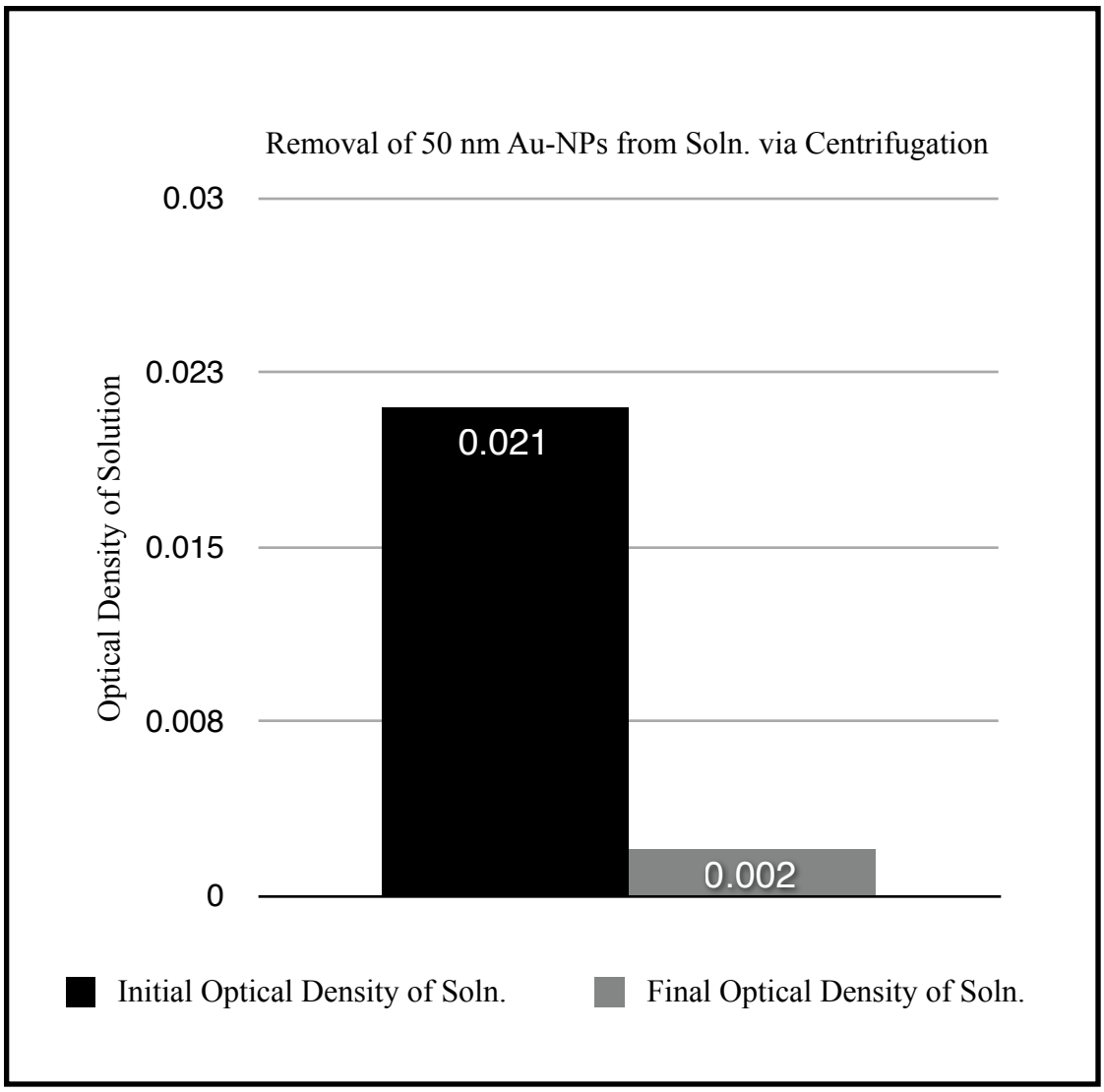

Figure 19. Removal of 50 nm Au-NPs from Solution via Centrifugation - UV-Vis Spectrometry Data

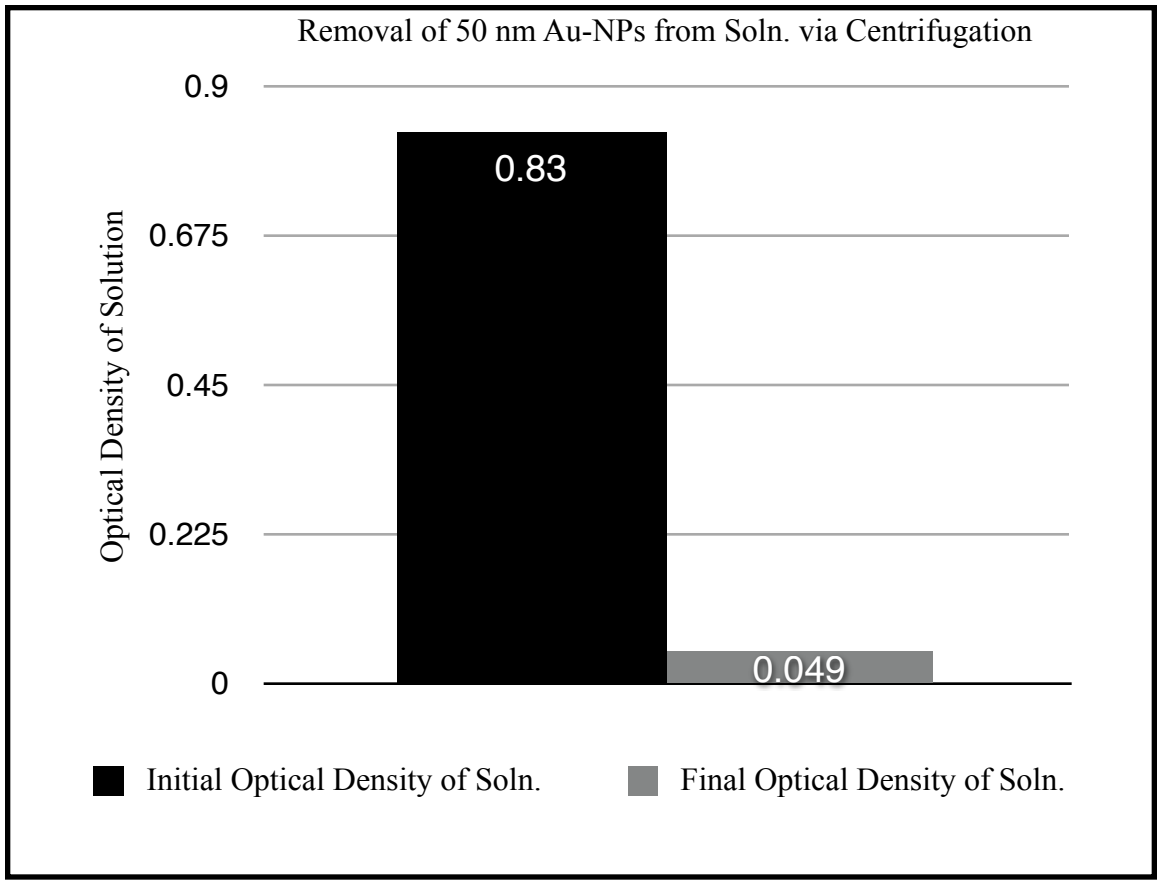

Figure 20. Removal of 50 nm Au-NPs from Solution via Centrifugation - GFAAS Spectrometry Data

Phase II - 10 nm Au-NP Studies

Objective

The objectives of the 10 nm Au-NP study are identical to those previously mentioned in Phase I (p.34). Colloidal Au-NPs for this portion of the study were obtained from Sigma Aldrich.

Results from this study are diagramed in Figure 21 and discussed in detail in Chapter XI.

Experimental

Fifteen milliliters of 1X PBS were transferred to a 50 mL centrifuge tube and combined with 8 mL of 10 nm Au-NPs. This solution was gently inverted. The optical density of the solution was measured by way of UV-Vis Spectrometry at 530 nm. Solution contents were then centrifuged at conditions optimized for the collection of F87G cells. The optical density of the supernatant was remeasured following centifugation in order to detect for Au-NPs remaining in solution.

Experimental Results

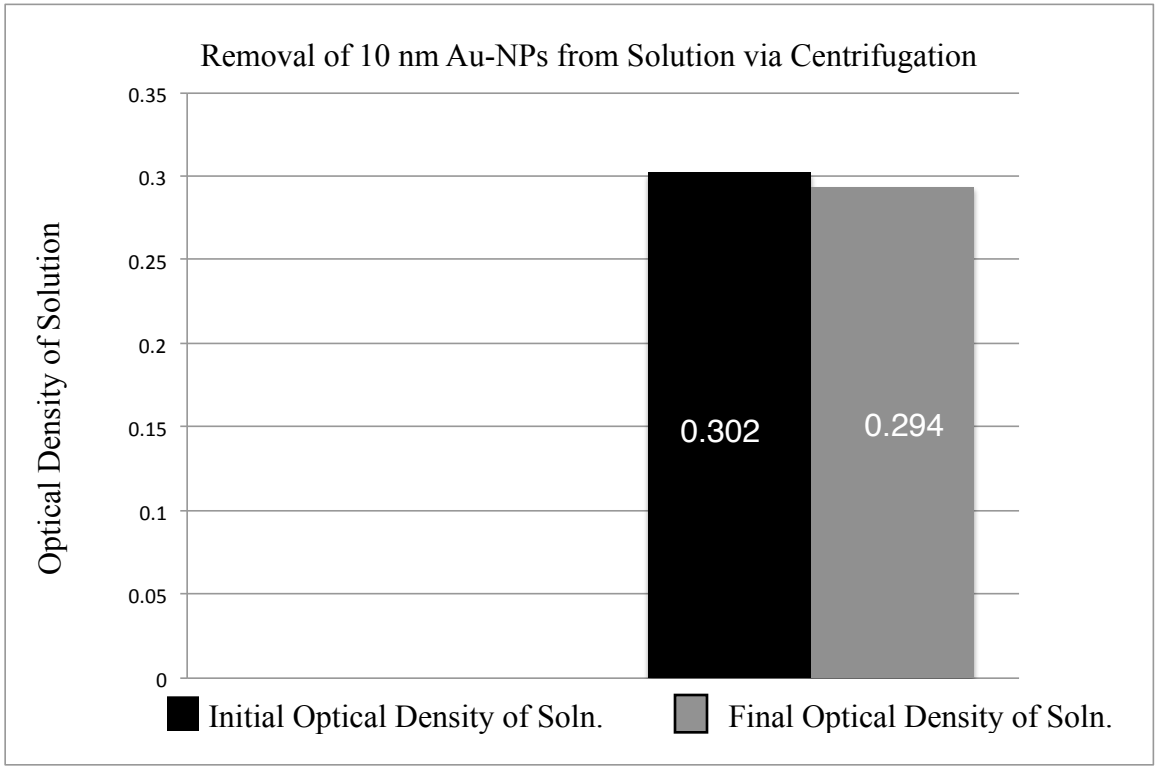

Figure 21. Removal of 10 nm Au-NPs from Solution via Centrifugation - UV Vis Spectrometry Data

Phase III - Examining the Cellular Uptake of Bare Au-NPs

Objective

Having determined optimal centrifugation conditions that would point toward the uptake of 10 nm Au-NPs into the F87G cell line, we moved into dosing studies. F87G cells were dosed with varying amounts of 10 nm Au-NPs and their lysate examined in order to quantify the amount of Au-NP uptake.

Results from this study are diagramed in Figures 22 & 23 and discussed in detail in Chapter XI.

Experimental

A stock solution of F87G cell culture was prepared by adding 1.75 mL of bacteria to 35 mL of TBM within a culture flask and incubated at 37 ˚C / 90 rpm. Cells were harvested at an optical density of 0.2 - 0.3, just before the point of exponential bacterial growth (see Figure 14). Following incubation, the cell culture was centrifuged at 6000 rpm / 35 min. / 4 ˚C in order to collect and remove debris from the cell culture.

Immediately following centrifugation, the supernatant was removed from the sample and cells were resuspended with 35 mL of fresh TBM. The optical density was again measured at this point to ensure that an OD of 0.2 - 0.3 was present following the collection of cells.

Five sampling flasks were prepared as outlined in Table 1.

	Tube One	Tube Two	Tube Three	Tube Four	Tube Five
F87G Cells	5.0 mL	5.0 mL	5.0 mL	5.0 mL	5.0 mL
Ampicilin	0.5 mL	0.5 mL	0.5 mL	0.5 mL	0.5 mL
Au-NPs	0 mL	0.125 mL	0.25	0.5 mL	1.00 mL
TBM	4.5 mL	4.375 mL	4.25 mL	4.0 mL	3.5 mL
Total Volume	10 mL	10 mL	10 mL	10 mL	10 mL

Table 1. Dosage Levels of Bare 10 nm Au-NPs

Each sampling flask was incubated at 37 ˚C / 90 rpm for 24 hours. Following the 24-hour incubation period samples were transferred into separate 25 mL centrifuge tubes and placed in an ice bath in preparation for centrifugation. Cells were centrifuged at 6000 rpm / 4 ˚C /10 min. in order to collect cellular content.

The supernatant of each sample was removed with care so as not to disrupt the cellular pellet. Three milliliters of cold 1X PBS were added to each sample in the same manner. The addition of PBS aliquots was repeated twice in order to wash each sample a total of three times.

Cellular digestion of each sample was carried out using concentrated Nitric Acid (69% TraceSELECT grade from Fluka Analytical). Three-hundred microliters of HNO_3 were added to each sample and digested overnight in a 60 ˚C sand-bath. The following day, 2 uL of lysate was removed, diluted in 400 uL of HNO_3 and analyzed via the GFAAS system.

Experimental Results

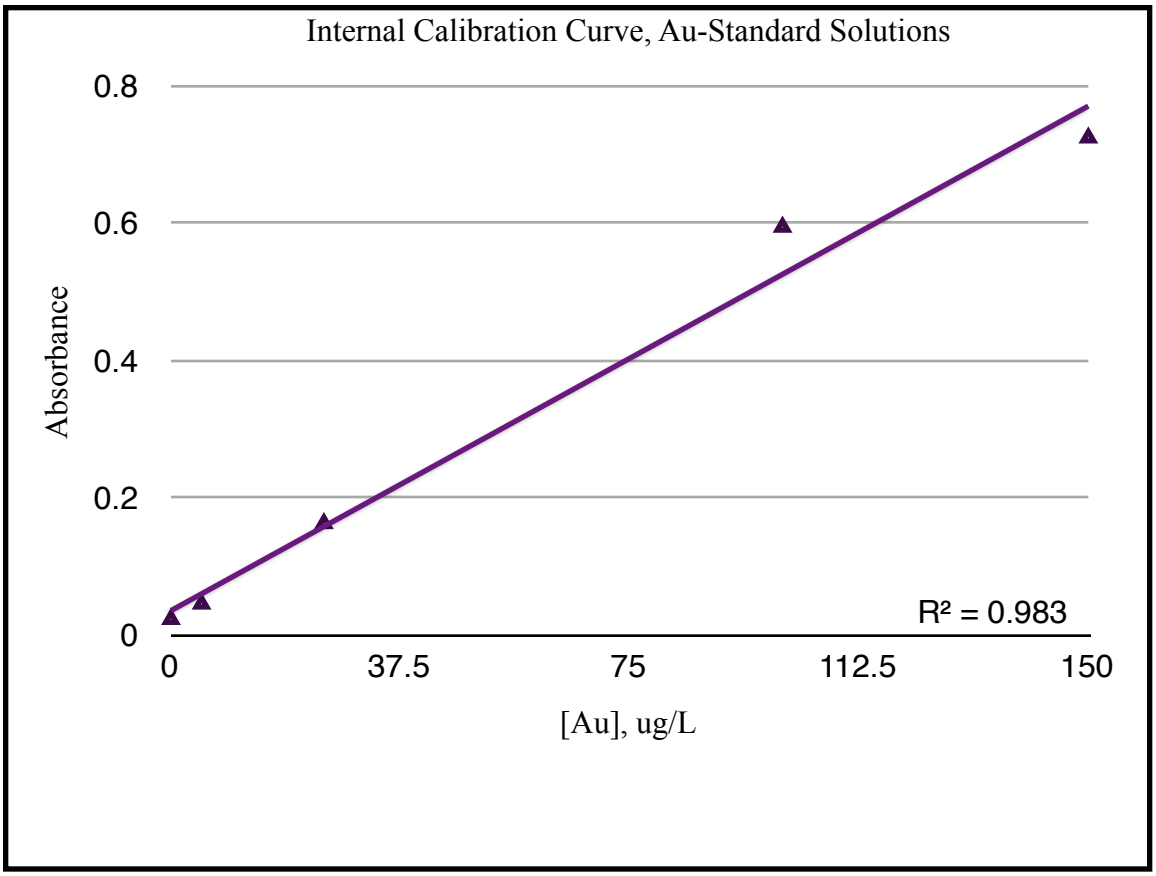

Figure 22. GFAAS Internal Calibration, Au-Standard Solutions

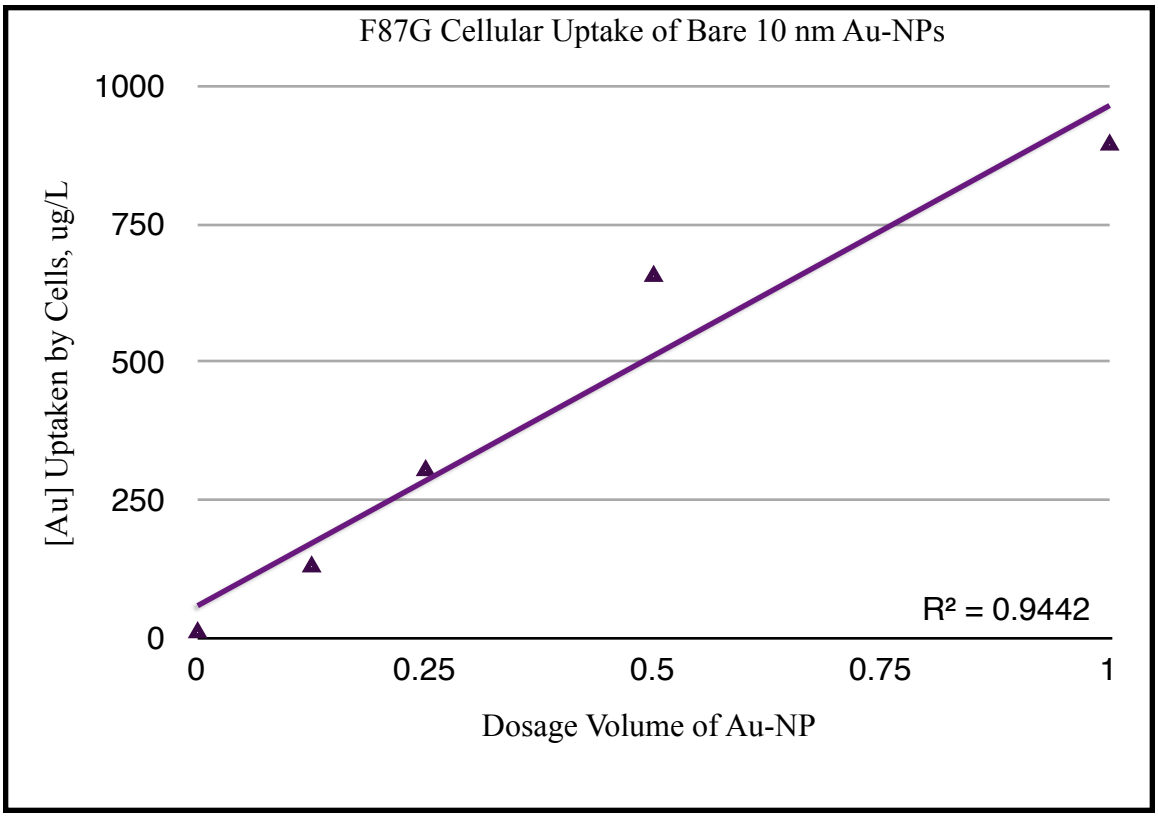

Figure 23. Cellular Uptake of Bare 10 nm Au-NPs by F87G Cell Line

Phase IV - Examining the Cellular Uptake of Protein-Coated Au-NPs

Objective

In the final phase of cellular uptake studies, the aim was to examine cellular uptake differences as related to BSA coated 10 nm Au-NPs and to determine, if any, the role of plasma protein in the uptake of colloidal gold.

Results from this study are diagramed in Figures 24 & 25 and discussed in detail in Chapter XI.

Experimental

A stock solution of F87G cell culture was prepared by adding 1.75 mL of bacteria to 35 mL of TBM within a culture flask and incubated at 37 ˚C / 90 rpm. Cells were harvested at an optical density of 0.2 - 0.3, just before the point of exponential bacterial growth. Following incubation, the cell culture was centrifuged at 6000 rpm for 35 minutes at 4 ˚C in order to collect and remove debris from the cells.

Immediately following centrifugation, the supernatant was removed from the sample and cells were resuspended with 35 mL of fresh TBM. The optical density was again measured at this point to ensure that an OD of 0.2 - 0.3 was present following the collection of cells.

Diluent (NANOPure water), BSA protein and 10 nm Au-NPs were premixed in said order in order to allow for the complexation of nanoparticle and protein before dosing into the cells. Each premixed solution was then added into individual sampling flasks according to the molar ratios of BSA:Au-NP outlined in Table 2 and Table 3.

	Sample 1 (0:1)	**Sample 2 (1:1)**	**Sample 3 (5:1)**	**Sample 4 (125:1)**	**Sample 5 (625:1)**	**Sample 6 (3125:1)**
Diluent	0.375 mL	0.025 mL	0.025 mL	0.025 mL	0.025 mL	0.025 mL
BSA*	0 mL	0.35 mL	0.35 mL	0.35 mL	0.35 mL	0.35 mL
Au-NPs	.125 mL	0.125 mL	0.125 mL	0.125 mL	0.125 mL	0.125 mL
F87G Cells	5.0 mL	5.0 mL	5.0 mL	5.0 mL	5.0 mL	5.0 mL
Ampicillin	0.5 mL	0.5 mL	0.5 mL	0.5 mL	0.5 mL	0.5 mL
TBM	4.0 mL	4.0 mL	4.0 mL	4.0 mL	4.0 mL	4.0 mL
VOL_{tot}	10 mL	10 mL	10 mL	10 mL	10 mL	10 mL

Table 2. Dosage Levels of Protein Coated Au-NPs, BSA:Au-NP (x:1)
* BSA solutions for the nanoparticle-protein premix were separately formulated to reflect outlined BSA to Au-NP molar ratios. Each premix solution was then brought to the same total volume of 0.5 mL.

	Sample 1 (0:2)	**Sample 2 (5:2)**	**Sample 3 (125:2)**	**Sample 4 (625:2)**	**Sample 5 (3125:2)**
Diluent	0.250 mL	0.025 mL	0.025 mL	0.025 mL	0.025 mL
BSA*	0 mL	0.35 mL	0.35 mL	0.35 mL	0.35 mL
Au-NPs	0.250 mL	0.125 mL	0.125 mL	0.125 mL	0.125 mL
F87G Cells	5.0 mL	5.0 mL	5.0 mL	5.0 mL	5.0 mL
Ampicillin	0.5 mL	0.5 mL	0.5 mL	0.5 mL	0.5 mL
TBM	4.0 mL	4.0 mL	4.0 mL	4.0 mL	4.0 mL
VOL_{tot}	10 mL	10 mL	10 mL	10 mL	10 mL

Table 3. Dosage Levels of Protein Coated Au-NPs, BSA:Au-NP (x:2)
* BSA solutions for the nanoparticle-protein premix were separately formulated to reflect outlined BSA to Au-NP molar ratios. Each premix solution was then brought to the same total volume of 0.5 mL

Each sampling flask was incubated at 37 ˚C / 90 rpm for 24 hours. Following the 24-hour incubation period samples were transferred into separate 25 mL centrifuge tubes and placed in an ice bath in preparation for centrifugation. Cells were centrifuged at 6000 rpm / 10 min. / 4˚C in order to collect cellular content.

The supernatant of each sample was removed and the cellular content was resuspended using 3 mL of cold 1X PBS. Three milliliter aliquots of PBS was added two additional times while also resuspending collected F87G cells.

The cellular digestion of each sample was carried out using concentrated Nitric Acid (69% TraceSELECT grade from Fluka Analytical). Three-hundred microliters of HNO_3 was added to each sampling tube and digested overnight in a 60 ˚C sand-bath. The following day, 2 uL of lysate was removed, diluted in 400 uL of HNO_3 and analyzed via the GFAAS system.

Experimental Results

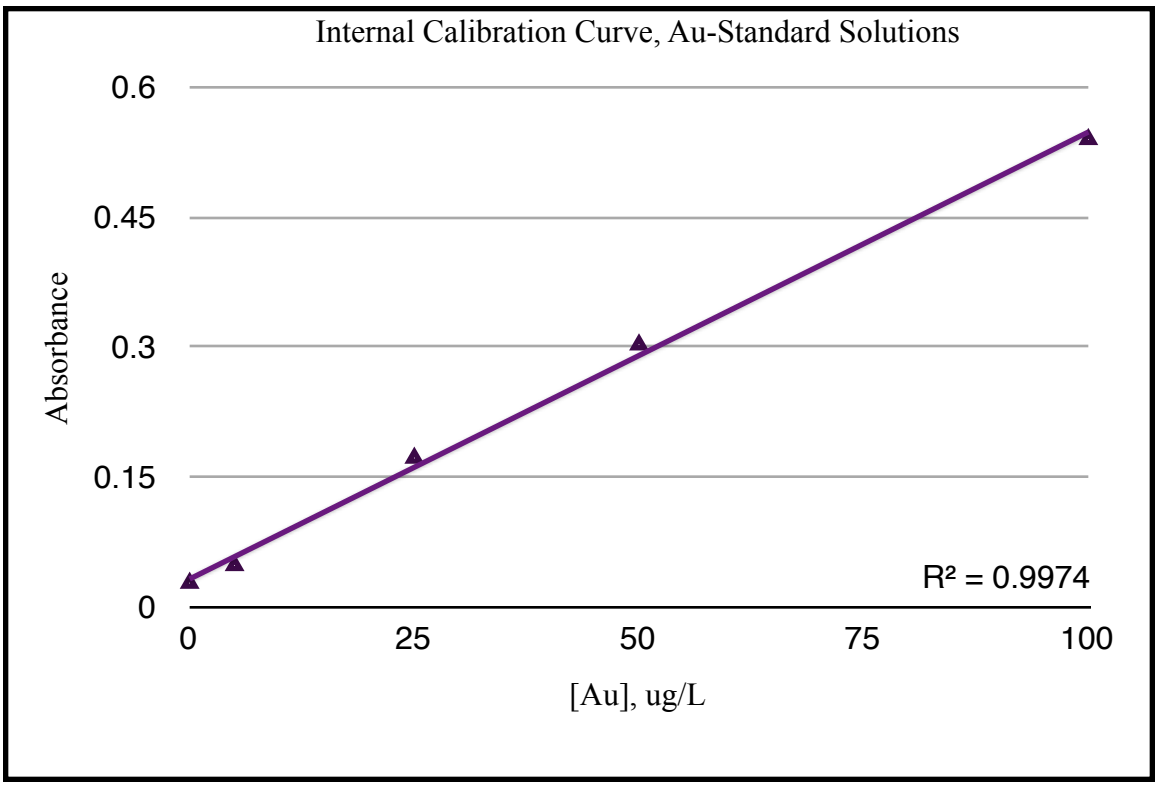

Figure 24. GFAAS Internal Calibration, Au-Standard Solutions

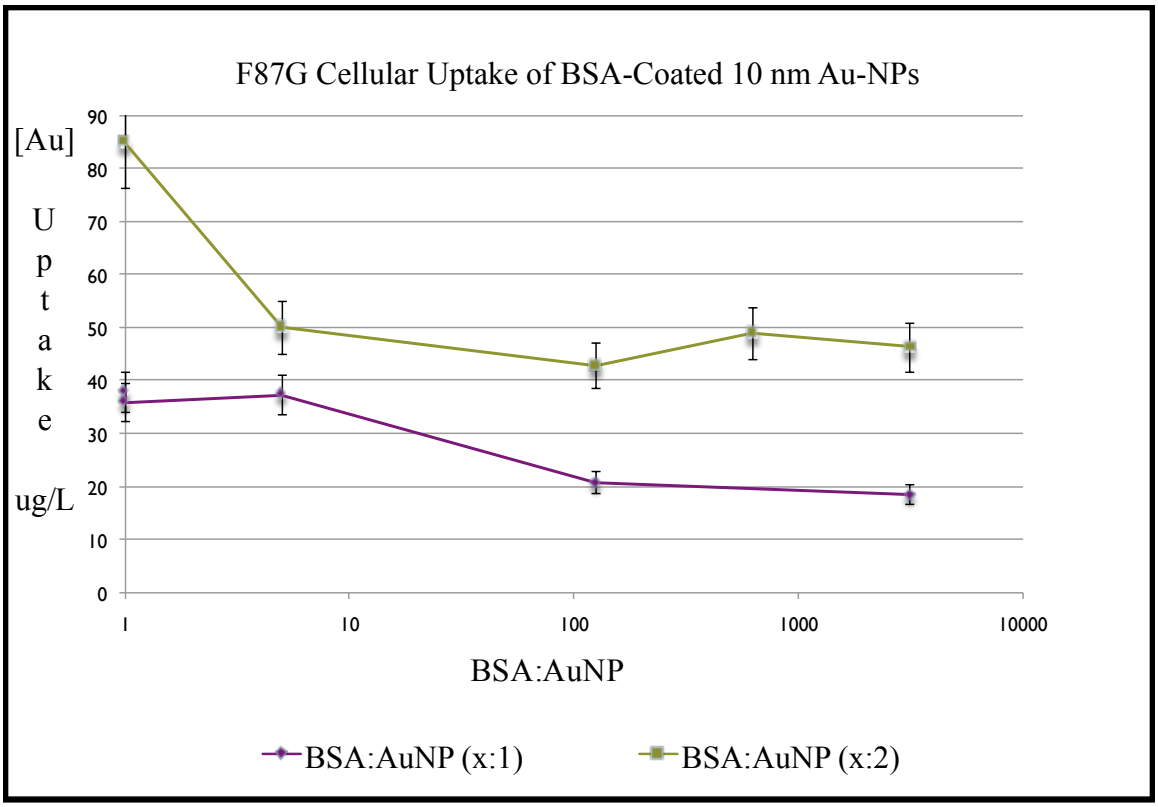

Figure 25. Cellular Uptake of BSA Coated 10 nm Au-NPs by F87G Cell Line

CHAPTER XI

OVERALL IMPLICATIONS

Investigative Observations

Host Cell Formation and Lysis

The F87G cell line cultured and used as the host cell within this experiment proved to be a viable vehicle for the cellular uptake of 10 nm Au-NPs, as is shown in Figure 23. Owing to the minimal disruption of F87G cells via sonication—we were only able to achieve a maximum 40% recovery of cellular lysate using homogenization techniques (Figures 15 & 16)—this cell line necessitates chemical digestion.

While the use of Nitric Acid digestion techniques proved efficient in the aforementioned experimental methods, it may present complications in the digestion of nanoparticles which require more sensitive / non-chemical lysing methods. In such cases, it may be beneficial to first explore the viability of a non-chemical digestion procedure as investigated in this study.

Nanoparticle-Protein Complexation

As previously noted, the complexation of nanoparticle and protein was not directly investigated within this study but rather confirmed through literature references. In attempts to quantify the presence of Au-NP in complexed solutions of nanoparticle and protein, UV-Vis Spectrometry proved inefficient. Owing to the intrinsic concentration of gold in our available colloidal solutions (5% w/v), such instrumentation failed to detect for the analyte.

While the aforementioned results failed to account for the presence of Au-NP within formed nanoparticle-protein complexes, information was obtained in regard to quantification techniques.

Examination of Cellular Uptake

In both Phase I and Phase II of the cellular uptake protocols, we aimed to determine a centrifugation speed wherein Au-NPs remained suspended in solution while F87G cells were maximally collected. Such would indicate a cellular uptake of Au-NPs versus a gravitational depression due to spinning conditions.

Studies were performed using 50 nm and 10 nm Au-NPs. As shown in Figures 19 & 20, Au-NPs of the 50 nm diameter were maximally collected under conditions

optimized for F87G cell collection. According to UV-Vis Spectrometry and GFAAS data, a maximal 9.52% of Au-NPs remained suspended in solution following centrifugation. Alternatively, a parallel study with 10 nm Au-NPs indicated a maximal 97.3% of Au-NPs remaining in solution following centrifugation. Such results point toward the cellular uptake of Au-NPs into F87G cells rather than centrifugal suppression.

Furthermore, the mass difference between Au-NPs and F87G bacterial cells is such that centrifugation would disallow a conclusion pointing toward simple adhesion. If the cellular uptake of Au-NPs occurs then the mass of Au-NP containing cells will be, by default, greater. As such, these cells can easily be separated out by gravitational force. In determining the centrifugation condition that does not remove Au-NPs from the supernatant but rather a maximum amount of bacterial cells from solution, we have specified the optimal spinning speed for 10 nm Au-NPs that points toward uptake rather than gravitational effects in the presence of F87G cells.

Having determined optimized centrifugation conditions for 10 nm Au-NPs, cellular uptake studies were first performed using bare Au-NPs. As shown in Figure 23, there is a direct and dose-dependent uptake of Au-NPs by the F87G cell line. Moreover, the F87G cell line can be said to have a high capacity for the uptake of colloidal gold

nanoparticles—at the highest dosing level, F87G cells are shown to ingest 894 ug / L of Au-NP.

In an effort to explicate the role of plasma proteins in the uptake of Au-NPs and their ability, if any, to mediate cellular entry, studies were performed using BSA coated Au-NPs as cellular dosing material. A number of variant protocols were performed—molar ratios of BSA and Au-NP were manipulated; duplicate samples were prepared to test for precision; and cellular content, following an extended incubation period, was washed and resuspended in order to facilitate maximal Au-NP uptake. Results from this study, as shown in Figure 25, indicate a suppression of Au-NP cellular uptake in the presence of bovine serum albumin plasma protein.

In arriving at said reasoning, two sample sets of BSA:Au-NP were prepared and examined in terms of cellular uptake. Sample set 1 was formulated using (x:1) molar ratios of plasma protein to Au-NP. Sample set 2 was formulated using (x:2) molar ratios of plasma protein to Au-NP. In each set, there is a significant decrease in Au-NP cellular uptake, indicating the inhibitory effects of BSA.

Future Directions

Owing to the nature of results obtained for protein coated Au-NPs, future research efforts aim to examine the *specific* interactions had between Au-NPs and select plasma

proteins. As is known, the nanoparticle-protein interface is yet to be fully understood and persists as a barrier in biological applications [2]. In turn, subsequent investigations propose to elucidate 1) the mechanism of Au-NP entry into the cell 2) optimal BSA:Au-NP saturation levels for cellular uptake and 3) intrinsic binding affinities and / or kinetics of nanoparticle-protein complexation. Results from these studies will help to expound data, as collected within this experiment, and provide information concerning optimal parameters in regard to cellular uptake and nanoparticle-protein interactions.

In the interest of time, current work has involved the investigation of bovine serum albumin, known to be the most abundant amongst plasma proteins. Subsequent studies, however, may prove additionally informative should protein identities be varied. Moreover, nanoparticle size and incubation periods can be manipulated so as to affect cellular uptake rates [25]. Proposed work, alongside the data collected within this study, will, in turn, continue to advance applications of nanomaterials while also elucidating their nature in complex biochemical systems.

REFERENCES

1. De Paoli Lacerda, S.H.; Park, J.J.; Meuse, C.; Pristinski, D.; Becker, M.L.; Karim, A.; Douglas, J.F. *ACS Nano* **2010** 1, 365

2. Shemetov A.; Nabiev I.; Sukhanova A. *ACS Nano* **2012** 6, 4585

3. Roco, M.C. *Nanoscience, Engineering and Technology* **2007**

4. Palmberg, C.; Dernis, H.; Miguet, C.; *Statistical Analysis of Science, Technology and Industry* **2009**

5. OECD. *Nanotechnology Innovation – An Overview* **2008**

6. Reddy, R. *Gold Nanoparticles: Synthesis and Applications* **2006**, 1791

7. Mody V.; Siwale R.; Singh A.; Mody R.; *Pharmacy & Bioallied Sciences* **2010** 2, 282

8. Tong L.; Wei Q.; Wei A.; Cheng JX. *Photochemical Photobiology* **2009** 85, 21

9. Kumar A.; Zhang X.; Liang Xing-Jie. *Biotechnology Advances* **2012**

10. Greenwood, R.; Kendall, K. *European Ceramic Society* **1999** 4, 479

11. Hackley, V. *Nanoparticle Standards at NIST: Gold Nanoparticle Reference Materials and Their Characterization* **2012**

12. Waniska, R.; Shetty, J.K.; Kinsella, J. E. *Agricultural and Food Chemistry* **1981** 29, 826

13. Nitta K.; Numata K.; *International Journal of Molecular Sciences* **2013** 14, 1629

14. Minor, W.; *Mol. Immunology*. **2012** 52, 174

15. Aubin-Tam M.E.; Hamad-Schifferli, K. *Biomedical Materials* **2008**, 3, 034001

55

16. Monopoli, P.; Walczyk, D.; Campbell, A.; Elia, G.; Lynch, I.; Bombelli F.; Dawson K. A.; *American Chemical Society* **2011** 133, 2525

17. Lundqvist, M.; Stigler, J.; Cedervall, T.; Berggard, T.; Flanagan, M. B.; Lynch, I.; Elia, G.; Dawson, K. *ACS Nano* **2011** 5, 7503

18. Tsuji J. S.; Maynard A. D.; Howard P. C.; James, J.T.;Chiu-Wing, L.; Warheit D.B.; Santamaria, A. B. *Toxicological Sciences* **2006** 89, 42

19. Nel, A. E.; Madler, L.; Velegol, D.; Xia, T.; Hoek, E. M. V.; Somasundaran, P.; Klaessig, F.; Castranova, V.; Thompson, M. *Nature Materials* **2009** 8, 54

20. Verma, A.; Uzun, O.; Hu, Y.; Hu, Y.; Han, Hee-Sun; Watson, N.; Chen, S.; Irvine, D. J.; Stellacci, F. *Nature Materials* **2008** 7, 588

21. Rejman, J.; Oberle V.; Zuhorn I. S.; Hoekstra D. *Biochem.* **2004** 377, 159

22. Rappoport, J.; Preece, J.; Chipman, K. Web Review. http://www.maths-in-medicine.org/uk/2011/nanoparticles/description.pdf **2011**

23. Thompson, J.; The Reaction of Alternate Oxidants with Cytochrome P450BM3 and Mutants Generates Spectrally Detectable, High Valent Iron Intermediates. M.S. Thesis, The University of North Carolina at Greensboro, Greensboro, NC, **2006**

24. Skoog, D.; Holler, F.J.; Crouch, R.; Thomson Brooks/Cole: CA; *Principles of Instrumental Analysis* **2010**

25. Soenen, S.J.; Manshian, B.; Montenegro, J. M.; Amin, F.; Meermann, B.; Thiron, T.; Cornelissen, M.; Vanhaecke, F.; Doak, S.; Parak, W. J.; et al. *ACS Nano* **2012** 6, 5767 56